PRAMANA
— journal of
physics

Vol. 64, No. 6
June 2005
pp. 927–937

Pattern formations in chaotic spatio-temporal systems

YING ZHANG[1], SHIHONG WANG[2], JINHUA XIAO[2], HILDA A CERDEIRA[3], S CHEN[4] and GANG HU[1,5,*]

[1]Department of Physics, Beijing Normal University, Beijing 100875, China
[2]Department of Basic Science, Beijing University Posts & Telecommunications, Beijing 100876, China
[3]The Abdus Salam International Centre for Theoretical Physics, P.O. Box 586, 34100 Trieste, Italy
[4]Institute of Applied Physics and Computational Mathematics, Beijing 100088, China
[5]Beijing–Hong Kong–Singapore Joint Center of Nonlinear and Complex Systems, Beijing Normal University Branch, Beijing, China
[*]Corresponding author. E-mail: ganghu@bnu.edu.cn

Abstract. Pattern formations in chaotic spatio-temporal systems modelled by coupled chaotic oscillators are investigated. We focus on various symmetry breakings and different kinds of chaos synchronization–desynchronization transitions, which lead to certain types of spontaneous spatial orderings and the emergence of some typical ordered patterns, such as rotating wave patterns with splay phase ordering (orientational symmetry breaking) and partially synchronous standing wave patterns with in-phase ordering (translational symmetry breaking). General pictures of the global behaviors of pattern formations and transitions in coupled chaotic oscillators are provided.

Keywords. Chaotic pattern formation; symmetry breaking; partial chaos synchronization.

PACS Nos 05.45.Xt; 05.45.Jn

1. Introduction

In the last half century, pattern formation has attracted great attention in many fields, such as hydrodynamics, optics, chemical reaction diffusion systems, biological systems and so on. The investigations of Turing patterns [1], dissipative structures [2], synergetic self-organizations [3,4] and other pattern formation topics have stimulated continual interest in nonequilibrium statistics and thermodynamics as well as nonlinear science [5–8]. For theoretical studies most previous work has focused on pattern formations from various regular media, such as stationary and homogeneous media, spatially or temporally periodic media, or other more complicated but still regular media. With these systems, we have been familiar with different classes of

instabilities or bifurcations leading to diverse interesting spatio-temporally ordered patterns [1–8].

In the last few decades the issue of chaos in spatio-temporal systems has become one of the central issues in nonlinear science [9–18]. Due to its random-like behavior, spatio-temporal chaos has also been an important topic in statistical physics. Other interesting problems arise in the context of spatio-temporal chaos: how ordered patterns can be formed from chaotic media; how various instabilities of chaos play essential roles in determining different types of pattern formations from chaos; how the concepts of chaos and pattern orders can be compatible with each other; and whether there are some general rules governing the variations from chaos to pattern formations. Most of the above problems have not been well answered so far, though some of them have been studied recently [9–18]. In this invited paper we discuss pattern formations from chaotic spatio-temporal systems modelled by coupled chaotic oscillators with a finite system size. We show that various ordered patterns can emerge from chaos via bifurcations characterized by different synchronization and desynchronization transitions, and some symmetry breakings and symmetry recoverings are associated with these transitions and pattern formations. In particular, we find that interesting periodic rotating wave patterns with splay phase ordering can appear from desynchronous spatio-temporal chaos via orientational symmetry breaking; and partially synchronous standing wave patterns with in-phase ordering and mirror symmetry can emerge from synchronous chaos via an instability of translational symmetry breaking. General pictures of global behaviors of pattern formations and transitions of coupled chaotic oscillators by varying coupling intensity are provided.

2. Model, symmetries and patterns

Let us consider the following model of coupled Rossler oscillators:

$$\begin{aligned}
\dot{x_i} &= -y_i - z_i + \varepsilon(x_{i+1} + x_{i-1} - 2x_i), \\
\dot{y_i} &= x_i + ay_i + \varepsilon(y_{i+1} + y_{i-1} - 2y_i), \\
\dot{z_i} &= b + (x_i - c)z_i + \varepsilon(z_{i+1} + z_{i-1} - 2z_i), \\
x_{i+N} &= x_i, \quad y_{i+N} = y_i, \quad z_{i+N} = z_i, \quad i = 1, 2, ..., N.
\end{aligned} \tag{1}$$

We take a set of particular parameters $a = 0.45$, $b = 2.0$, and $c = 4.0$ at which the single Rossler oscillator is chaotic with the chaotic attractor given in figure 1a. We focus our investigation on the system with size $N = 6$, which is large enough to show many interesting spatio-temporal behaviors of pattern formations and transitions, and is sufficiently small for performing detailed numerical computations and mathematical analyses easily on the system dynamics and statistics. Extensions to other sizes and even to other spatio-temporal chaotic systems will be discussed in the last section.

We can start our investigation from two extreme cases. One is $\varepsilon = 0$, at which the six oscillators evolve according to the single Rossler dynamics, with trajectories

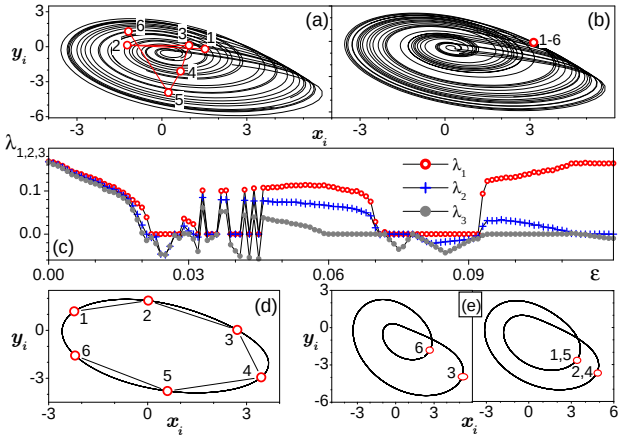

Figure 1. Simulations of eq. (1) for $a = 0.45$, $b = 2.0$, $c = 4.0$ and $N = 6$. The same parameters are used in all the following figures unless specified otherwise. The numbers in the figures indicate the positions of the given oscillators at an arbitrary instant. (**a**) $\varepsilon = 0$. All the six oscillators share the same chaotic attractor with randomly distributed phases. (**b**) $\varepsilon = 0.12 > \varepsilon_c = 0.111$. All the six oscillators have identical attractor and asymptotically synchronous trajectory. (**c**) The largest three Lyapunov exponents plotted vs. ε. Computations for different εs are performed from different randomly chosen initial conditions. (**d**) $\varepsilon = 0.085$. A stable periodic rotating wave pattern with splay phase distribution $\mathbf{r}_{i+1}(t) = \mathbf{r}_i(t + T/6)$. T is the period of the motion. (**e**) $\varepsilon = 0.085$. A stable periodic partially synchronous standing wave pattern with in-phase angle distribution and mirror symmetry. Sites 1 and 5 (2 and 4) have an identical trajectory. The trajectories of site 3, pair $(1, 5)$, pair $(2, 4)$, and 6 are different. Sites $1, 2, 4$, and 5 have identical orbit, and sites 3 and 6 have a same orbit too. Sites 3 and 6 play the role of the axis for the mirror symmetry. Note, figures 1d and 1e are obtained for identical system parameters but with different initial conditions.

independent (desynchronous) of each other (figure 1a). The other is $\varepsilon > \varepsilon_c = 0.111$, at which all the six oscillators follow again the single Rossler dynamics, with all the six trajectories fully synchronous with each other (figure 1b). It is interesting to note that both the completely synchronous state at $\varepsilon > \varepsilon_c$ and the completely desynchronous state at $\varepsilon = 0$ satisfy full spatial symmetry in the sense that the system behavior is invariant for any exchanges $i \rightleftharpoons j$, $i, j = 1, 2, ..., 6$ and both states are regarded to be completely symmetric. However, the natures of symmetries of the two states are essentially different. For the synchronous state we have

$$\mathbf{r}_i(t) = \mathbf{r}_j(t), \quad i, j = 1, 2, ..., 6; \ \mathbf{r}_i(t) = (x_i(t), y_i(t), z_i(t)), \tag{2}$$

i.e., the full symmetry is satisfied exactly at any time while for the desynchronous state we have

$$\mathbf{r}_i(t) \neq \mathbf{r}_j(t),$$

$$\langle A(\mathbf{r}_i(t))\rangle = \langle A(\mathbf{r}_j(t))\rangle, \quad i,j = 1,2,...,6,$$

$$\langle A(\mathbf{r}_i(t))\rangle = \lim_{T\to\infty} \frac{1}{T}\int_0^T A(\mathbf{r}_i(t))\,\mathrm{d}t, \tag{3}$$

where $A(\mathbf{r}_i(t))$ is an arbitrary function of the system variables of the ith site. We call eq. (2) a dynamical symmetry and eq. (3) a statistical symmetry.

Equations (2) and (3) define full dynamical and statistical symmetries, respectively, consisting of various partial symmetries. In this paper we are interested in the following three kinds of symmetries.

(i) Translational symmetries: The system behaviors remain unchanged when they are viewed from site i and site $i+m$, $i,m = 1,2,...,6$.
(ii) Mirror symmetry: The system behaviors remain unchanged when they are viewed from site $i+m$ and site $i-m$, $i,m = 1,2,...,6$ with i being a fixed mirror axis.
(iii) Orientational symmetry: The system behaviors are identical when they are viewed from clockwise and anticlockwise orientations.

All partial symmetries (i)–(iii) can also be classified as dynamical symmetries and statistical symmetries as we do in eqs (2) and (3). It is obvious that both the completely synchronous state ($\varepsilon > \varepsilon_c$) and completely desynchronous state ($\varepsilon = 0$) satisfy all the symmetries (i)–(iii).

The dynamical and statistical behaviors of system (1) are very rich and interesting in the coupling region $0 < \varepsilon < \varepsilon_c$. In figure 1c we plot the three largest Lyapunov exponents from arbitrary initial conditions, and the plots look rather complicated. In figures 1d and 1e we show the asymptotic patterns of the system, starting from two arbitrarily chosen initial conditions, for coupling $\varepsilon = 0.085$. Spatially well-ordered and temporally periodic patterns are observed. A significant point is that both patterns have different partial symmetries. The former (rotating wave, $\mathbf{r}_{i+1}(t) = \mathbf{r}_i(t+\frac{T}{6})$ with T being the period of the system, $i = 1,2,...,6$) keeps the translational symmetry but breaks the orientational and mirror symmetries, and the latter (partially synchronous standing wave, $\mathbf{r}_1(t) = \mathbf{r}_5(t)$, $\mathbf{r}_2(t) = \mathbf{r}_4(t)$, with sites 3 and 6 being the mirror axis) keeps the mirror and orientational symmetries but breaks the translational symmetry. It is interesting to ask how the essentially different ordered patterns of figures 1d and 1e can emerge from spatio-temporal chaos. In §§3 and 4 we study these problems by varying ε from the region near $\varepsilon = 0$ to the region $\varepsilon > \varepsilon_c$.

3. Variations from desynchronous chaos and emergence of rotating wave patterns

In figure 2a we plot again the three largest Lyapunov exponents $\lambda_1 \geq \lambda_2 \geq \lambda_3$ by using the following plotting approach. We start from the computation for $\varepsilon = 0$, and increase ε in steps of size $\Delta\varepsilon = 0.001$. For each ε we run eq. (1) by taking the ending state for the previous ε as the initial condition for the current coupling, i.e., we pursue the branch of variation starting from the high-dimensional spatio-temporal

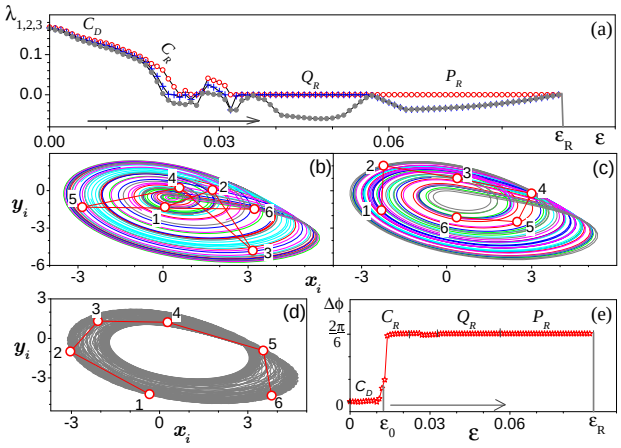

Figure 2. The variations of the system state by continuously increasing ε from 0. (**a**) The three largest Lyapunov exponents. After $\varepsilon > \varepsilon_{\rm R} = 0.09$, this branch jumps to the branch of figure 3a. (**b**) Disordered chaos ($C_{\rm D}$) for $\varepsilon = 0.005$. (**c**) Chaotic rotating wave with splay phase ordering ($C_{\rm R}$), $\varepsilon = 0.014$. (**d**) Quasi-periodic rotating wave ($Q_{\rm R}$), $\varepsilon = 0.04$, which transits to the periodic rotating wave of figure 1d by further increasing ε. (**e**) $\Delta\phi$ defined in eq. (7) plotted vs. ε. A phase transition from random phase $\Delta\phi = 0$ to splay phase $\Delta\phi = 2\pi/6$ is observed around $\varepsilon_0 \approx 0.012$.

chaos of $\varepsilon = 0$. Now, the behavior of figure 2a is considerably simpler than that of figure 1c, showing a clear tendency of decreasing chaoticity and increasing spatial ordering with an increase of ε.

In figure 2a the notation $C_{\rm D}$ represents disordered chaos; and $C_{\rm R}$, $Q_{\rm R}$ and $P_{\rm R}$ represent chaotic, quasi-periodic, and periodic rotating waves, respectively. All these patterns emerge one after the other as $C_{\rm D} \to C_{\rm R} \to Q_{\rm R} \to P_{\rm R}$ in the course of increasing ε, through successive phase transitions and bifurcations. The asymptotic trajectories of these characteristically different states are shown in figures 2b–2d and figure 1d. In figure 2b, the $C_{\rm D}$ state is chaotic in time and disordered in space. In the $C_{\rm R}$ state of figure 2c the phases of the six oscillators are well-ordered though the state is still chaotic. The $C_{\rm R}$ state can vary from high-dimensional chaos (with six positive Lyapunov exponents) to low-dimensional chaos (with a single positive Lyapunov exponent) by increasing ε. In figure 2d, the $C_{\rm R}$ state transits, by passing some complicated bifurcations in a small parameter window, to a state $Q_{\rm R}$ quasi-periodic in time and phase ordered in space. This quasi-periodicity is replaced by a periodic rotating wave state $P_{\rm R}$ (figure 1d) by further increasing ε.

Figure 2 shows transitions: disordered chaos → splay phase ordered chaos → splay phase ordered quasi-periodicity → splay phase ordered periodicity, among which we are familiar with the last two transitions while the first phase transition is new and significant. This transition shows how spatial order can appear from disorder through spontaneous orientational symmetry breaking. To show this transition we define phase angle of a site as

$$tg\ \phi_i(t) = \frac{y_i(t)}{x_i(t)}. \tag{4}$$

By setting $\phi_1 = 0$ and computing

$$\Delta\phi_{i,i+1} = \lim_{n\to\infty} \frac{1}{n} \sum_{m=1}^{n} \Delta\phi_{i,i+1}(m),$$

$$\Delta\phi_{i,i+1}(m) = \phi_{i+1}(m) - \phi_i(m), \tag{5}$$

where $\phi_i(m)$ is the phase angle of the ith oscillator at time $m\Delta t$, Δt is the time interval between successive measurements which is chosen to be 0.1. $\Delta\phi_{i,i+1}(m)$ takes values in $(-\pi, \pi)$, and this uniquely determines $\Delta\phi_{i,i+1}$. In figure 2e we plot $\Delta\phi = |\Delta\phi_{1,2}|$ vs. ε. We find $\Delta\phi = 0$ in the $C_{\rm D}$ state and

$$\Delta\phi = \frac{2\pi}{6} \tag{6}$$

for all $C_{\rm R}$, $Q_{\rm R}$ and $P_{\rm R}$ states. A spatial state, satisfying the condition $\Delta\phi = 2\pi k/N$, with k a nonzero integer and N the system size, is called a splay phase state. Two interesting points are found in figure 2e. First, there is indeed a phase transition at $\varepsilon = \varepsilon_0 \approx 0.012$ characterized by the sudden change from $\Delta\phi = 0$ (random phase) to $\Delta\phi = 2\pi/6$ (splay phase ordering). Second, from the point view of space symmetry, the $C_{\rm D}$ state has complete symmetry (in the sense of statistics) while $C_{\rm R}$, $Q_{\rm R}$ and $P_{\rm R}$ states possess splay phase ordering and orientational symmetry breaking. The spatial order and symmetry breaking observed in figure 1d originates early at the phase transition from $C_{\rm D}$ chaos to $C_{\rm R}$ chaos. On the contrary, transitions from $C_{\rm R}$ chaos to $Q_{\rm R}$ quasi-periodicity and then to $P_{\rm R}$ periodicity change the temporal behavior of the system state only, but not essentially the spatial ordering.

The mechanism underlying the emergence of the splay phase ordering transition at ε_0 can be well-understood, based on the competition of two facts, chaos and coupling. Chaos always has a tendency to make phase distributions of different oscillators random, while mutual coupling is in favor of certain phase orders. Mutual coupling in eq. (1) provides a gradient force yielding an effective potential, which can be heuristically written as

$$H(\phi) \approx \sum_{i=1}^{N} \frac{1}{2}\varepsilon r^2[(\sin\phi_{i+1} - \sin\phi_i)^2 + (\cos\phi_{i+1} - \cos\phi_i)^2]$$

$$\approx \varepsilon r^2 \left[N - \sum_{i=1}^{N} \cos\Delta\phi_{i,i+1}\right], \tag{7}$$

$$x_i(t) = r_i\cos\phi_i(t), \quad y_i(t) = r_i\sin\phi_i(t), \quad r^2 \approx r_i^2, \quad i = 1, 2, ..., N.$$

In eq. (7) we neglect the amplitude fluctuations and the fluctuation of the z_i variables. The gradient force intends to bring the oscillators to certain phase distributions determined by the minima of the potential (7). It is easy to show that at the phase distributions

$$\Delta\phi_{2,1} = \Delta\phi_{3,2} = \cdots = \Delta\phi_{n,n+1} = \Delta\phi = \frac{2\pi k}{N}, \quad |k| = 0, 1, 2, ..., \leq N/2 \tag{8}$$

the potential $H(\phi)$ has extrema ($\frac{\partial H}{\partial \phi_i} = 0$), and the necessary and sufficient condition for any such extrema to be minima is

$$\cos\Delta\phi > 0, \quad \Delta\phi < \frac{\pi}{4}. \tag{9}$$

Now the picture of how the rotating wave of figure 1d appears through the orientational symmetry breaking and various bifurcations becomes clear. For very small ε ($\varepsilon < \varepsilon_0$) chaos dominates, producing random phase distribution $\Delta\phi = 0$. As the coupling increases the potential basins of eqs (8) and (9) increase their attracting intensions. The transition point $\varepsilon = \varepsilon_0$ is determined by the balance of the effects of chaotic randomizing and coupling ordering of the most favorable basin. It is emphasized that the in-phase state $k = 0$, $\Delta\phi = 0$ always satisfies the conditions of eqs (8) and (9). However, this state requires too strict a synchronization condition, and needs large coupling to balance the chaotic randomizing effect. For small ε, one always first finds the splay phase state with $\Delta\phi \neq 0$ if eqs (8) and (9) can be satisfied for some nonzero ks. This is why the rotating wave (if it exists) can be found only in the branch starting from $\varepsilon = 0$.

4. Variations from synchronous chaos and emergence of partially synchronous standing wave patterns

By varying ε from 0 to ε_{R} we cannot find the pattern of figure 1e. For further exploring the dynamical behavior of system (1) we vary ε from the completely synchronous state. In figure 3a we do exactly the same as in figure 2a by decreasing ε from ε_{c} (some small noise is applied to test the stability of the synchronous state). The Lyapunov spectra in figure 3a are again different from figure 1c. Therefore, we find two different branches of pattern transition sequences, one is demonstrated by increasing ε from 0 (figure 2a) which is stopped at $\varepsilon = \varepsilon_{\mathrm{R}} = 0.090$, and the other by decreasing ε from ε_{c} (figure 3a) which is ended at $\varepsilon = \varepsilon_{\mathrm{L}} = 0.056$. At ε_{R} (ε_{L}) the branch of figure 2a (figure 3a) jumps to the branch of figure 3a (figure 2a) for $\varepsilon > \varepsilon_{\mathrm{R}}$ ($\varepsilon < \varepsilon_{\mathrm{L}}$). In figure 3a, the motions CSC, PSC, PSP, and PSQ represent the Completely Synchronous Chaotic state (as figure 1b), Partially Synchronous Chaotic state, Partially Synchronous Periodic state (i.e., standing wave, as figure 1e), and Partially Synchronous Quasi-periodic state, respectively.

In figure 3a the variations from CSC of figure 1b to PSP of figure 1e are clearly shown. As ε decreases below ε_{c}, the CSC state becomes unstable via a long-wave ($k = 1$) instability. Slightly below ε_{c} the system should be replaced by a desynchronous state of mode $k = 1$ which is closest to the CSC state. The only state having such properties is a partially synchronous chaotic state with mirror symmetry. This is the case observed in figures 3b and 3c where an interesting mirror symmetric structure of *abcbad* emerges. The oscillators of 1–6 perform four distinctive chaotic trajectories $a(t)$ (sites 1 and 5), $b(t)$ (sites 2 and 4), $c(t)$ (site 3) and

$d(t)$ (site 6), respectively. The two pairs of sites $(1, 5)$ and $(2, 4)$ take identical trajectories, i.e., keep pair chaos synchronizations after the full synchronization breaks at ε_c.

In figures 3b and 3c, sites 3 and 6 play a role of mirror symmetry axis in the ring of coupled oscillators. From CSC of figure 1b to PSP of figures 3b and 3c we observe a bifurcation from homogeneous chaos synchronization with full symmetry to structured partially synchronous chaos with partial (mirror) symmetry, and translational symmetry breaks in this transition. From figures 3b and 3c to figure 1e the PSC chaotic state transits to the PSP partially synchronous periodic standing wave state through a tangent bifurcation. This bifurcation changes the temporal behavior of the state only, but does not affect the spatial order and symmetry structure.

To conclude the discussion of §§3 and 4 two new and significant points should be emphasized. First, in both variations from the chaotic states of figures 1a and 1b to the regular and periodic patterns of figures 1d and 1e, we find that the symmetry breakings and spatial orderings emerge not at the transitions from chaos to periodicity but at the transitions from chaos to chaos (i.e., disordered desynchronous chaos to splay phase ordered desynchronous chaos in figure 2c associated with orientational symmetry breaking, and full synchronous chaos to partial synchronous chaos in figure 3b associated with translational symmetry breaking). Second, in the variation branch of figure 2a we find $\Delta\phi = 2\pi/6$ for all splay phase states, while in the branch of figure 3a we find uniquely in-phase states $\Delta\phi = 0$, which will be shown and further discussed in the next section.

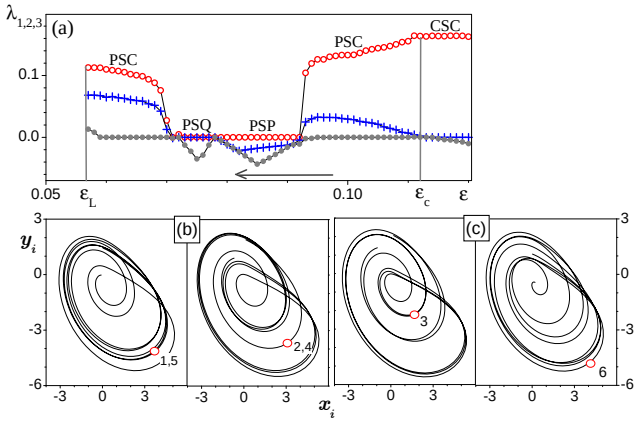

Figure 3. The variations of the system state by decreasing ε from ε_c. (**a**) The same as figure 2a with ε decreased. After $\varepsilon < \varepsilon_L = 0.056$, this branch jumps to the branch of figure 2a. (**b**), (**c**) $\varepsilon = 0.098$. The partially synchronous chaotic pattern with in-phase ordering and mirror symmetry, which transits to the periodic standing wave figure 1e with spatial ordering and symmetry structure unchanged.

5. Global picture of pattern formations and transitions in coupled chaotic oscillators

Though the behavior in figure 1c looks rather complicated, the general features of pattern formations and pattern transitions by varying ε are clearly understood from the discussions of the above two sections. To better understand the general features of state variations, we plot, in figure 4a, $\Delta\phi$ vs. ε for both variations of increasing ε from 0 (arrows to right) and decreasing ε from ε_c (arrows to left). It is remarkable that the complicated variations of the three Lyapunov exponents in figure 1c is now replaced by the considerably simpler hysteresis loop of the phase angle distributions, from which the global picture of bifurcations and the structure of pattern formations in six coupled chaotic oscillators can be fully understood. The new and essential points in figure 4a can be summarized as follows:

(i) By increasing ε from 0, one first find desynchronous high-dimensional chaos with random phase distribution ($\Delta\phi = 0$) for small ($\varepsilon < \varepsilon_0$) coupling. As ε increases over the critical value ε_0, the disordered and desynchronous chaos transits to another type of desynchronous chaos with spatial ordering having average equal phase shift $2\pi/6$ between neighboring oscillators, associated with an orientational symmetry breaking. This is a novel kind of chaotic phase synchronization, and this transition creates the so-called splay phase structure serving as the original reason for the emergence of the periodic rotating wave pattern of figure 1d. This splay phase chaos can further bifurcate to splay phase quasi-periodic and then splay phase periodic (rotating wave) states with the spatial ordering unchanged (the upper branch of figure 4a).

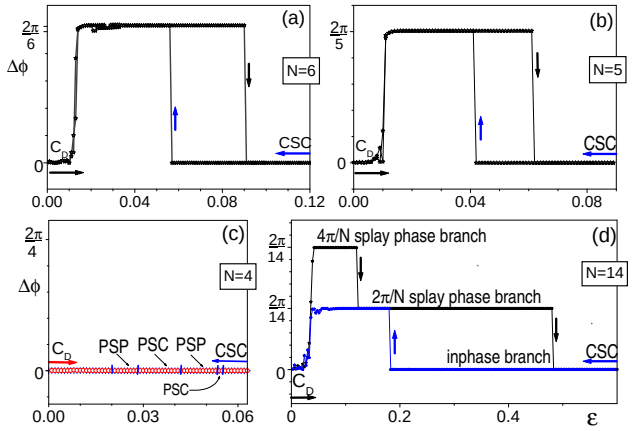

Figure 4. (**a**) Average phase difference between adjacent oscillators, $\Delta\phi$, plotted vs ε. $N = 6$. (**b**) The same as (a) with system size $N = 5$. (**c**) The same as (a) with $N = 4$. Splay phase state, rotating wave and hysteresis loop no longer exist for $N \leq 4$. (**d**) The same as (a) with $N = 14$. Two hysteresis loops indicate coexistence of two splay phase modes $k = 1$ (middle branch of $\Delta\phi = 2\pi/14$) and $k = 2$ (upper branch of $\Delta\phi = 4\pi/14$).

(ii) By decreasing ε from ε_c, the synchronous chaos desynchronizes to inhomogeneous chaos with partial synchronization determined by a spatial structure of mirror symmetry with a mirror axis spontaneously appearing via translational symmetry breaking. This partially synchronous chaos can further bifurcate to partially synchronous quasi-periodic and periodic patterns with again the spatial ordering of mirror symmetry (together with the fixed mirror axis) unchanged. All states in this branch (lower branch indicated by left arrows) have angle relation $\Delta\phi = 0$, the so-called in-phase angle distributions. It is emphasized that the in-phase state of PSC and the disordered phase state $\Delta\phi = 0$ for $\varepsilon < \varepsilon_0$ are different in nature. In the former case chaotic phase locking yields the in-phase synchronization of $\Delta\phi = 0$ while in the latter case randomly distributed phases cause $\Delta\phi = 0$.

(iii) The upper branch (the lower branch) is ended at $\varepsilon = \varepsilon_R$ ($\varepsilon = \varepsilon_L$). As ε increases (decreases) over ε_R (ε_L), the upper branch (lower branch) jumps to the lower branch (upper branch) through a first-order phase transition. It is interesting to note that at the transition from one branch to the other, the state changes its multiple symmetries simultaneously (at ε_R translational and mirror symmetry breakings and orientational symmetry recovering, and the opposite at ε_L), and these transitions should be of the first order leading to the hysteresis loop since, generically, no continuous transition can exchange multiple symmetries at a single bifurcation point. However, all transitions and bifurcations within a same branch change one kind of spatial symmetry or do not change spatial symmetry, and they can be of the second order without difficulty.

Some general conclusions about the behavior of figure 4a can be drawn. First, from the theory of eqs (7)–(9), the features of figure 4a may be observed for all system sizes of $N \geq 5$. In figure 4b we do the same as figure 4a with $N = 5$, and find similar behaviors like figure 4a. Second, from eq. (9), the splay phase states and rotating wave solutions cannot exist for $N \leq 4$. Consequently, the hysteresis loop between the in-phase and splay phase branches does not exist for systems with $N < 5$. In figure 4c we plot $\Delta\phi$ vs. ε for $N = 4$, where the absence of the whole splay phase branch and the hysteresis fully confirms the prediction of eq. (9). Therefore, $N = 5$ is the minimum number of oscillators allowing rotating wave solution of figure 1d. Third, from eqs (8) and (9) multiple hysteresis loop may be observed for $N > 8$ since different splay phase states, $2\pi k/N$ for $k = 1, 2, ...$, may be stable with the condition $(2\pi k/N) > (\pi/2)$ satisfied. In figure 4d we do the same as in figure 4a with $N = 14$; now the multiple hysteresis loops verify the coexistence of bistable splay phase patterns of $k = 1$ and $k = 2$. The lower branch ($\Delta\phi = 0$, arrows to the left) represents in-phase patterns, which may be chaotic, quasi-periodic and periodic and may be completely synchronous ($\varepsilon > \varepsilon_c$) and partially synchronous with mirror symmetry ($\varepsilon_L < \varepsilon < \varepsilon_c$); the middle branch ($\Delta\phi = 2\pi/14$) and the upper branch ($\Delta\phi = 4\pi/14$) represent modes $k = 1$ and $k = 2$ splay phase patterns, respectively. Again we find the disordered spatio-temporal chaos ($\varepsilon < \varepsilon_0$) first transits to splay phase chaotic states (both $k = 1$ and $k = 2$), and these splay phase orderings finally lead to periodic rotating wave patterns of $k = 1$ and $k = 2$ by further increasing ε.

We have investigated many other chaotic spatio-temporal systems, and found that the bifurcation and pattern formation pictures of figures 2–4 exist commonly in

coupled chaotic oscillators, and most features in these figures can be found in general chaotic spatio-temporal systems such as coupled chaotic maps and chaotic partial differential equations. Further investigations in this direction may be of significance for understanding the problem of pattern formations from spatio-temporal chaos.

References

[1] A M Turing, *Philos. Trans. R. Soc. London, Ser. B.* **237**, 37 (1952)
[2] G Nicolis and I Prigogine, *Self-organization in nonequilibrium systems: From dissipative structures to order through fluctuations* (Wiley, New York, 1977)
[3] H Haken, *Synergetics* (Springer-Verlag, Berlin, 1977)
[4] S Kauffman, *The origins of order: Self-organization and selection in evolution* (Oxford University Press, New York, 1993)
[5] K J Lee, W D Mccormick, Q Ouyang and H L Swinney, *Science* **261**, 192 (1993)
[6] M C Cross and P C Hohenberg, *Science* **263**, 1569 (1994)
[7] T Yanagita and K Kaneko, *Physica* **D82**, 288 (1995)
[8] J M Ottino, F J Muzzio, M S Rudroff and I Rehberg, *Phys. Rev.* **E55**, 2742 (1997)
[9] L M Pecora, T L Carroll, G Johnson and D Mar, *Phys. Rev.* **E56**, 5090 (1997)
[10] G Hu, J Z Yang, W Q Ma and J H Xiao, *Phys. Rev. Lett.* **81**, 5314 (1998)
[11] L M Pecora and T L Carroll, *Phys. Rev. Lett.* **80**, 2109 (1998)
[12] L M Pecora, *Phys. Rev.* **E58**, 347 (1998)
[13] P Muruganandam, K Murali and M Lakshmanan, *Int. J. Bifurcat. Chaos* **9**, 805 (1999)
[14] A Pande and R Pandit, *Phys. Rev.* **E61**, 6448 (2000)
[15] G Hu, Y Zhang, H A Cerdeira and S Chen, *Phys. Rev. Lett.* **85**, 3377 (2000)
[16] M Zhan, G Hu, Y Zhang and D H He, *Phys. Rev. Lett.* **86**, 1510 (2001)
[17] X-L Qiu and P Tong, *Phys. Rev. Lett.* **87**, 094501 (2001)
[18] S Wang, J Xiao, X Wang, B Hu and G Hu, *Eur. Phys. J.* **B30**, 571 (2002)